

Article

Liquid Phase Furfural Oxidation under Uncontrolled pH in Batch and Flow Conditions: The Role of In Situ Formed Base

Alessandra Roselli ¹, Yuri Carvalho ², Franck Dumeignil ² , Fabrizio Cavani ¹ , Sébastien Paul ²  and Robert Wojcieszak ^{2,*} 

¹ Dipartimento di Chimica Industriale “Toso Montanari”, Università di Bologna, Viale Risorgimento 4, 40136 Bologna, Italy; alessandra.roselli@studio.unibo.it (A.R.); fabrizio.cavani@unibo.it (F.C.)

² Univ. Lille, CNRS, Centrale Lille, ENSCL, Univ. Artois, UMR 8181, UCCS, Unité de Catalyse et Chimie du Solide, F-59000 Lille, France; yuri.carvalho@centralelille.fr (Y.C.); Franck.dumeignil@univ-lille.fr (F.D.); sebastien.paul@centralelille.fr (S.P.)

* Correspondence: robert.wojcieszak@univ-lille.fr

Received: 7 December 2019; Accepted: 2 January 2020; Published: 3 January 2020



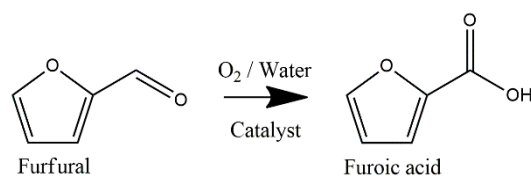
Abstract: Selective oxidation of furfural to furoic acid was performed with pure oxygen in aqueous phase under mild conditions and uncontrolled pH using hydrotalcite-supported gold nanoparticles as catalyst. Hydrotalcites with different Mg: Al ratios were tested as support. The effects of reaction time, temperature and furfural/catalyst ratio were evaluated. The catalyst Au/HT 4:1 showed the highest activity and selectivity to the desired product, achieving a complete conversion of furfural to furoic acid after 2 h at 110 °C. Further, stability tests were carried out in a continuous stirred-tank reactor and a progressive deactivation of the catalyst due to the leaching of Mg²⁺ cations from the support inducing changes in the pH of the reaction medium was observed.

Keywords: furfural; furoic acid; gold; hydrotalcite; oxidation

1. Introduction

The increase of the CO₂ emissions associated with the still increasing global production based on fossil resources is a source of motivation for researchers to find renewable feedstocks to produce chemicals and fuels. Within this frame, the conversion of biomass into fuels and top-valued chemicals is considered as one of the most attractive alternatives to the use of fossil resources [1]. Furfural (FF), the other name for 2-furaldehyde (C₅H₄O₂), is a hetero-aromatic furan ring with an aldehyde functional group. It is a natural precursor of furan-based chemicals and has high potential to become a major renewable platform molecule to produce biosourced chemicals and biofuels. Furfural is a natural product that can be easily obtained by dehydration of xylose, a monosaccharide found in large quantities in lignocellulosic biomass [2]. Industrial production of furfural started in 1922, when Quaker Oats Company gave destiny to oat hulls by processing them in a digester with sulphuric acid. Since then, around 50,000 tons per year of oat hulls were being transformed to furfural and sold for 25 cents a pound [3]. It was mainly used as a raw material for the production of other furanic compounds, such as insecticides or herbicides, and in lubricating oils and resins production. Furfural is one of the most promising platform molecules, not only because of its very reactive chemical structure but also because it can be further transformed into higher value-added molecules that find applications mainly as fuels or monomers for the polymers industry [4]. Through the catalytic selective oxidation of the furfural aldehyde moiety, it is possible to produce 2-furoic acid, which is the first down-line oxidation derivative of furfural having many applications in the pharmaceutical (esters forms [5]), agrochemical, flavour and fragrance industries. In the domain of resins, new routes for producing 5-hydroxyvaleric

acid from furoic acid can also be highlighted [6]. However, other products can also be obtained from furfural oxidation, such as maleic acid, succinic acid, 2(5H)-furanone and CO₂ [4,7]. Industrially, furoic acid (FA) is nowadays produced through Cannizzaro disproportionation reaction in aqueous NaOH [4]. However, this process presents some drawbacks since the disproportionation reaction also coproduces furfuryl alcohol, leading to maximal selectivity to furoic acid of 50%. Moreover, the final solution has to be neutralized with sulfuric acid, forming sodium bisulfate that must be separated and then treated or disposed. The Cannizzaro reaction is also highly exothermic, so that temperature control of the reactor must be implemented [4]. For these reasons, many studies were done to combine heterogeneous catalysis in presence of NaOH for improving the furfural conversion to furoic acid [8–11]. Within this frame, direct catalytic furfural oxidation using pure oxygen or, even better, air would open the gate to higher selectivity to furoic acid. Douthwaite et al. demonstrated that furfural selective oxidation to furoic acid could take place under base-free conditions when AuPd/Mg(OH)₂ was employed as a catalyst [12]. However, they also proved that AuPd/Mg(OH)₂ was not stable at low pH since Mg²⁺ leaching was detected when no NaOH was added [12]. Therefore, the high conversion observed under initially supposed base-free conditions was finally attributed to the in situ formation of a homogeneous Mg(OH)₂ base. However, no stability test was performed to verify any catalyst deactivation due to its dissolution in aqueous medium. Apart from furfural oxidation, many works in the literature describe the use of basic solid supports, such as MgO, CaO and hydrotalcites, to perform catalytic reactions in aqueous medium but not taking in consideration the connection between catalyst activity and instability related to soluble base formation [13–15]. Considering the use of MgO, the authors already observed the support leaching phenomena on furfural oxidation [16] and further studied the use of more stable oxides such as MnO₂ [17]. In the present work, a heterogeneously-catalyzed process to produce furoic acid by selective oxidation of furfural using different hydrotalcites-supported gold nanoparticles is proposed as an alternative to the Cannizzaro reaction. The reaction scheme is shown in Scheme 1. Further, the study of the stability of such catalysts was carried out in a continuous stirred-tank reactor (CSTR), and a relation between activity and catalyst stability was proposed.



Scheme 1. Reaction scheme of the catalytic oxidation of furfural to furoic acid.

2. Results

2.1. Catalysts Characterization

Hydrotalcite supports were prepared as described in the experimental section using a co-precipitation method. After calcination under static air at 500 °C during 3 h, the transformation of the hydrotalcite structure into MgO-Al₂O₃ mixed oxides occurred as shown by XRD (Figure 1). The XRD patterns exhibit the typical features of a mixed oxide of the Mg(Al)O type. The characteristic diffraction peaks clearly observed at $2\theta \approx 43^\circ$, 63° and also 36° correspond to the periclase phase (MgO, powder diffraction file 45-0946 from the International Centre for Diffraction Data, ICDD). In addition, the formation of spinel structures is not observed. Furthermore, the samples were found clean of any impurity such as residual nitrate salts.

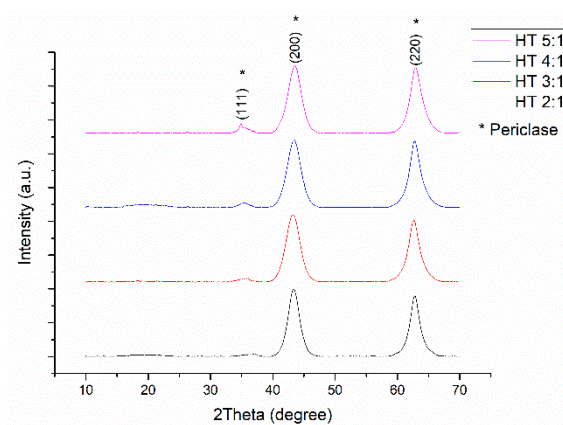


Figure 1. Hydrotalcites X-ray diffractograms after calcination of the samples.

After gold nanoparticles immobilization, the prepared samples were characterized again using XRD technique (Figure 2). The XRD patterns presented typical diffraction peaks from hydrotalcite (powder diffraction file 89-460 from ICDD). Due to hydrotalcite memory effect, it was able to recover its original structure upon rehydration of the mixed oxides when subjected to the gold nanoparticles immobilization protocol. However, it is still possible to observe the presence of periclase, by the appearance of the peaks at $2\theta \approx 43^\circ$ and 63° , which is more remarkable for the samples with higher Mg/Al ratio.

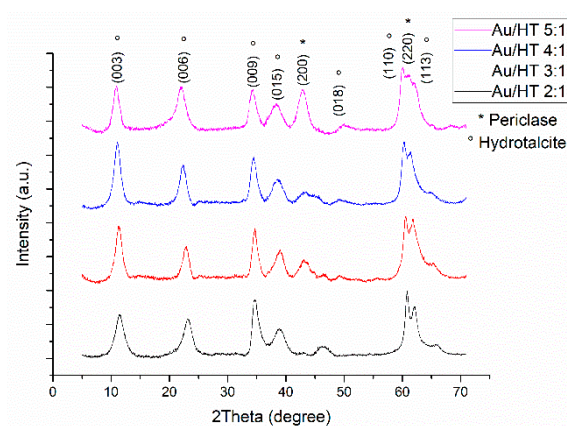


Figure 2. Au/HTs catalysts X-ray diffractograms.

ICP-OES analyses were performed for determining the actual gold content in each catalyst (theoretical value 2 wt.%) as well as the Mg/Al ratio for all the hydrotalcite supports (theoretical values 2, 3, 4 and 5). The Al, Au and Mg contents are displayed in Table 1. Au content in the catalysts was a bit lower than expected with a value of 1.4 ± 0.3 wt.%, while the samples contained a lower proportion of Mg that expected, with a deviation of ca. 20% compared to the theoretical value.

Table 1. ICP-OES analyses of the prepared catalysts.

Catalyst	Au (w/w %)	Al (w/w %)	Mg (w/w %)	Mg/Al Ratio
Au/HT 2:1	1.3%	13.8%	23.0%	1.7
Au/HT 3:1	1.7%	11.1%	27.8%	2.5
Au/HT 4:1	1.2%	8.7%	27.5%	3.2
Au/HT 5:1	1.4%	7.6%	30.0%	4

The Au/HT 4:1 catalyst was selected for characterization by TEM to determine the metal dispersion on the surface due to its performance (see below). TEM images and particle size distribution can be seen in Figure 3. The images showed that the gold nanoparticles are highly dispersed on the support surface. The particles sizes are distributed between 2.5 and 5.5 nm with an average particle size of 3.7 nm.

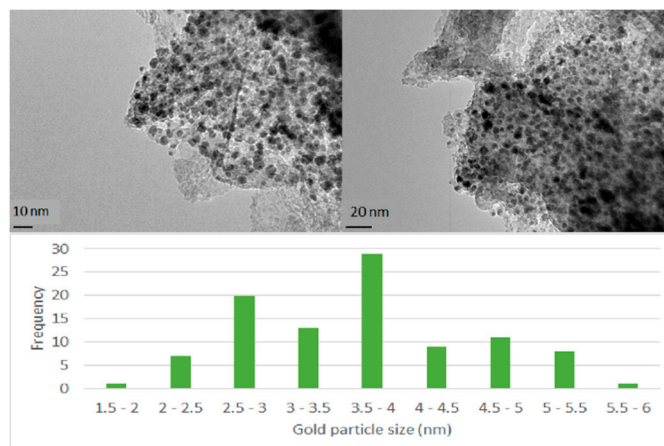


Figure 3. TEM images and particle size distribution from Au/HT 4:1.

The surface areas of the catalysts were determined using the BET model whereas the pore volumes were calculated using the BJH method. The results are given in Table 2. The surface area and pore volume clearly drop from the lowest Mg/Al ratio catalyst, Au/HT 2:1, to higher Mg/Al ratio catalysts. In addition, surface area and pore volume also drop when comparing the bare hydrotalcite support with the corresponding catalyst. For instance, surface area and pore volume for the bare HT 2:1 support were $91 \text{ m}^2\text{g}^{-1}$ and $0.33 \text{ cm}^3\text{g}^{-1}$, respectively, in comparison with $73 \text{ m}^2\text{g}^{-1}$ and $0.17 \text{ cm}^3\text{g}^{-1}$, respectively, after impregnation. It clearly shows the influence of the gold nanoparticles deposition method on the textural properties of the support.

Table 2. Textural properties.

Catalyst	BET Surface Area (m^2g^{-1})	Pore Volume (cm^3g^{-1})
Au/HT 2:1	73	0.17
Au/HT 3:1	25	0.07
Au/HT 4:1	30	0.08
Au/HT 5:1	25	0.07

Finally, to characterize the acid-base properties of the supports, TPD experiments were performed using either 10 mol.% NH_3 or CO_2 in He gas mixtures. The adsorption of the gas molecules were carried out at 50°C and 40°C , respectively, for 1 h. For desorption, the temperature ramp used was $10^\circ\text{C min}^{-1}$ up to 500°C , which is the calcination temperature used to prepare hydrotalcite supports [18]. The desorption curves of NH_3 for the different supports are shown in Figure 4.

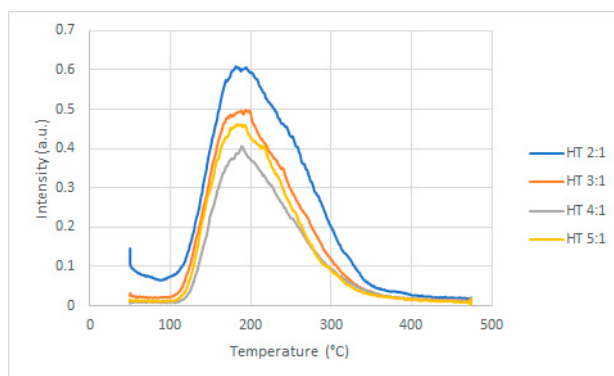


Figure 4. NH_3 desorption curves for the different HT supports.

As expected, the results obtained from NH_3 desorption are correlated with the Mg: Al molar ratios. The desorption curve in the case of HT Mg: Al = 2:1 catalyst is much more intense than for the other supports. This is probably due to the high surface area of this sample ($90 \text{ m}^2/\text{g}$) as compared to other samples. The HT 3:1 and 5:1 led to very close desorption curves while the HT 4:1 showed the least intense curve. It is also worth to note that all the HT supports seem to have only one kind of acid sites corresponding to desorption at low temperature (around 190°C), suggesting weak or weak to medium acid sites. Quite similar but reversed trend was observed for 2:1, 3:1 and 5:1 samples with CO_2 desorption data as shown in Figure S1. As expected, the HT Mg: Al = 5:1 support adsorbed more CO_2 than the other 2:1 and 3:1 HT samples, being the most basic support used in this study. The hydrotalcite samples seem to have two kinds of basic sites represented by the CO_2 desorption at different temperatures, the strongest at higher temperature (around 275°C) and the second one at lower temperature (around 120°C). Table 3 displays the amounts, in arbitrary units per gram of material, of NH_3 and CO_2 desorbed in TPD.

Table 3. Desorbed NH_3 and CO_2 amounts in TPD for HTs.

Support	NH_3 (a.u.g $^{-1}$) ¹	CO_2 (a.u.g $^{-1}$) ¹	Mg/Al Ratio
HT 2:1	90	33	1.7
HT 3:1	63	68	2.5
HT 4:1	48	—	3.2
HT 5:1	56	105	4

¹ Arbitrary units per gram of support.

2.2. Blank Test with Hydrotalcite Supports Only

The reaction was first performed with the bare hydrotalcites (without any gold) to check if the supports themselves were active in furfural oxidation (Figure 5). Up to 45% conversion was observed, however, the yield to furoic acid was not higher than 11%. The conversion could be attributed to the degradation of furfural into undetected byproducts, as no other oxidation products such as furfuryl alcohol could be detected, leading to a low carbon balance (always less than 80%). Without support the blank test done in the same conditions led to only 5% furfural conversion.

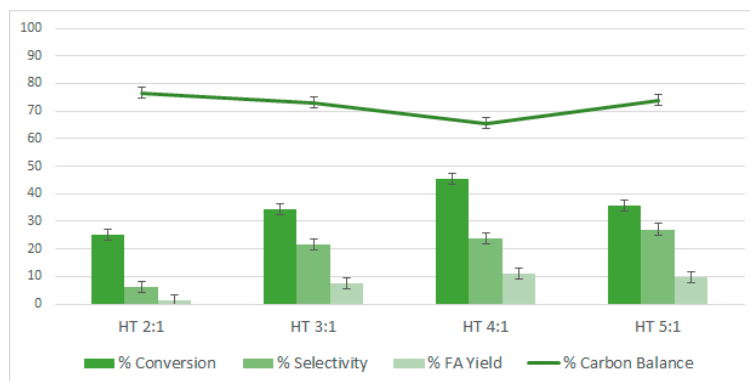


Figure 5. Comparison of the performance in furfural oxidation of HT supports with different molar Mg: Al ratios. Batch reactor, $p = 6$ bar (O_2), $t = 110$ °C, 2 h, stirring rate 600 rpm, [FF] = 26 mM, 100 mg of HT.

2.3. Reactivity of Gold Nanoparticles Supported on Hydrotalcites

Strong increases both in the FF conversion and the yield to furoic acid were observed using supported gold nanoparticles catalysts. Indeed, the gold-mediated oxidation is known to avoid radical pathways [19], thus, the degradation of furfural is less favoured as confirmed by the higher carbon balance (always close to or higher than 90%). At the same time, different Mg:Al molar ratios were evaluated to study whether the increase in the Mg content and correlated basic properties would result in an enhancement of the catalytic performances. Actually, increases in furfural conversion and furoic acid yield were observed as the Mg content in Au/HT increased as shown in Figure 6. Full conversion and selectivity to furoic acid were achieved with the Au/HT 4:1 and Au/HT 5:1 catalysts. This was probably due to an increase in the overall basicity of the support, which would promote the activity of the catalysts. Indeed, the catalytic results were well correlated with the basic properties of the HT supports. Obviously, the 100% yield to furoic acid (and hence the 100% carbon balance) means no degradation or formation of undesired products at all.

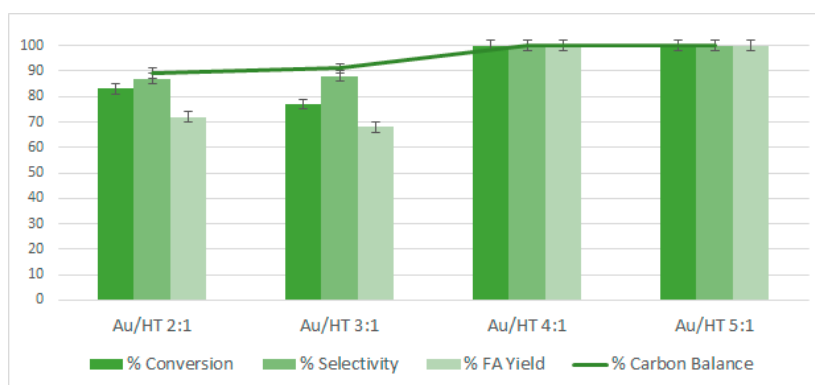


Figure 6. Comparison of the performance in furfural oxidation of Au/HT catalysts with supports having different molar Mg: Al ratios. Batch reactor, $p = 6$ bar (O_2), $t = 110$ °C, 2 h, 600 rpm, FF/Au molar ratio = 200:1, [FF] = 26 mM, 25 mg of catalyst.

2.4. Study on the Effect of the Reaction Time

The effect of the reaction time on catalytic activity was further studied using the Au/HT 4:1 catalyst. Complete furfural conversion was observed after 120 min of reaction as shown in Figure 7. The selectivity to furoic acid was above 90% in all cases. In addition, the carbon balance was above 90%, indicating minimum degradation of furfural in these conditions. It shows that the catalyst is very active even at short reaction times.

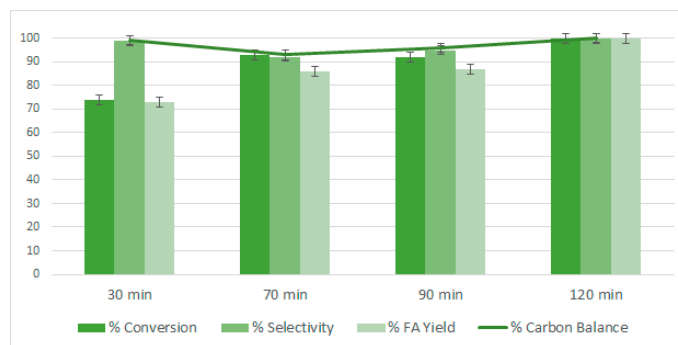


Figure 7. Effect of the reaction time using Au/HT 4:1. Furfural oxidation, batch reactor, $p = 6$ bar (O_2), $t = 110$ °C, 600 rpm, FF/Au = 80:1, [FF] = 26 mM, 63 mg of catalyst.

In addition, ICP-OES analyses of samples of the liquid phase were performed for monitoring if any leaching was taking place during the reaction. Table 4 shows the concentration of Au and Mg in the reaction medium for different reaction times (analysed twice at each time), as well as the pH value.

Table 4. ICP-OES analyses and pH of the reaction samples.

Time	[Au] mgL ⁻¹	[Mg] mgL ⁻¹	[Mg] _{leach.} /[Mg] _{total} w/w %	pH
0	—	—	0	3
30	—	13.4	1.55%	7
70	—	17.7	2.04%	7
90	—	19.8	2.29%	7
120	—	23.0	2.66%	7

According to ICP-OES no gold leaching was detected even after 2 h of batch reaction. However, the Mg concentration in the reaction medium constantly increased with the reaction time, indicating that some leaching occurs. In addition, the pH of all reaction samples was 7, which was not expected since both furfural and furoic acid solutions have a pH around 3 in a base-free medium. This is a strong evidence that a soluble base was formed in situ even if the Mg leaching was limited, as a 10 mgL⁻¹ increase of concentration was observed between 30 and 120 min of the reaction time.

2.5. Study on the Effect of the Temperature

The reaction was also studied regarding the influence of the temperature. The results are presented in Figure 8. At an FF/Au molar ratio of 80, the catalyst displayed full conversion, both at 110 and 130 °C, with high values of selectivity and carbon balance. However, at higher temperature (150 °C) some degradation of furfural occurred as illustrated by the lower carbon balance values. At 80 °C the conversion was not complete after 2 h of reaction.

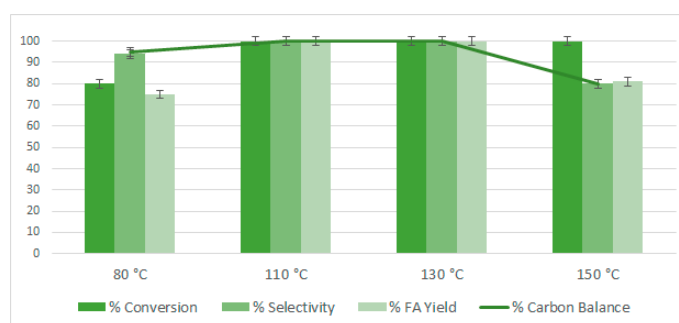


Figure 8. Effect of the reaction temperature using Au/HT 4:1. Furfural oxidation, batch reactor, $p = 6$ bar (O_2), 600 rpm, 2 h, FF/Au = 80, [FF] = 26 mM, 63 mg of catalyst.

2.6. Study of the Effect of the FF/Au Molar Ratios

Au/HT 4:1 was tested using three different theoretical molar ratios between furfural and gold: 80, 200 and 400. As can be seen in Figure 9, the catalyst showed full conversion and high furoic acid yield at low FF/Au molar ratios.

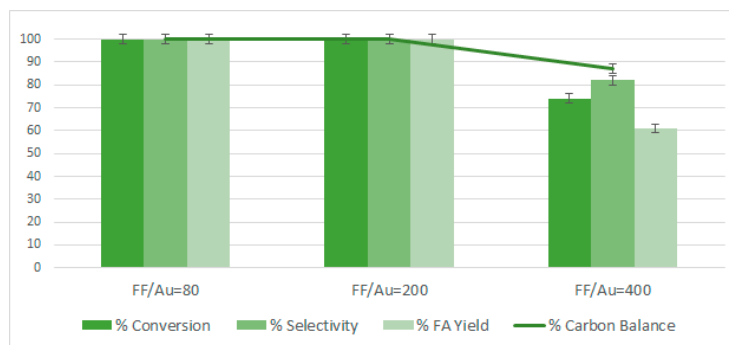


Figure 9. Effect of the FF/Au molar ratios using Au/HT 4:1 catalyst. Furfural oxidation, batch reactor, $p = 6$ bar (O_2), $t = 110$ °C, 600 rpm, 2h, [FF] = 26 mM.

2.7. Stability of Au/HT 4:1 in a Continuous Reactor

Following the results obtained from the ICP-OES analyses of the liquid sampled during the batch reactions and suspecting that some support leaching takes place, Au/HT 4:1 was tested in a continuous reactor (CSTR-type) working at a constant feed flow rate of 0.5 mL min^{-1} . The continuous reaction system allows a better monitoring of catalyst stability and suitability for potential industrial use. In this system, the reactant was pumped into the vessel and the solution under reaction was collected at the same flow rate, while the catalyst remained trapped inside the reactor by using a filter preventing any catalyst entrainment in the outflow. Figure 10 depicts the reaction behavior over 6 h of time on stream.

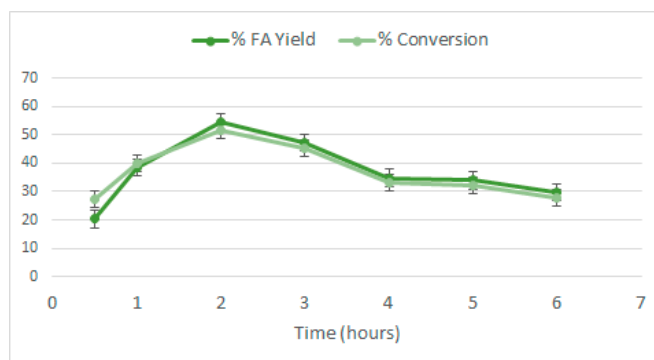


Figure 10. Furfural oxidation in CSTR employing Au/HT 4:1 as catalyst. $p = 5$ bar air; $t = 110$ °C; FF/Au = 50; feed: 0.5 mL min^{-1} [FF] = 26 mM; 100 mg of catalyst.

Initially, the catalyst seemed to have a relatively low activity, which increased progressively up to 2 h under stream and then constantly decreased. It can be seen that the selectivity to furoic acid and carbon balance were high during the whole reaction since the conversion, and yield values were very close. The steady state was not achieved during the 6 h on stream, indicating that deactivation was taking place in parallel, even during the transient state in the first hours. The pH of the outflow was measured for each reaction sample and was found constant at 7 all along the reaction, as it was observed for batch reaction. This means that leaching of the support was taking place constantly. It is proposed that homogeneous $Mg(OH)_2$ [12] is progressively released in the reaction medium and eliminated by the flow, then causing the activity fall down. One should also consider that for maintaining the pH at 7, the leaching phenomena should be stronger than in batch reaction, since a

fresh furfural solution (pH = 3) is being introduced continuously into the CSTR. As described before in the literature [12–15], it was believed that catalysts based on solid basic supports such as $\text{Mg}(\text{OH})_2$, MgO , CaO , hydrotalcites, etc., would promote base-free catalytic transformations in aqueous medium. However, this work, presents an evidence that catalysts based on hydrotalcite supports can be active in apparently base-free conditions but in reality, it is not the case because of their partial dissolution in the reaction medium, then generating in situ a soluble base.

3. Discussion

This work was conducted using water as solvent, pure oxygen or air as oxidants and gold nanoparticles immobilized on hydrotalcite (HT) supports. The aim was to develop a greener and sustainable process to selectively oxidize furfural to furoic acid. Using appropriate method, gold nanoparticles were immobilized on different HT supports. A study on the acid-base properties of the supports was done for different HT materials prepared with different Mg: Al molar ratios. Under mild conditions, the synergistic effect between gold nanoparticles and properties of the HT support, allowed a fast and complete transformation of furfural to furoic acid (100% yield). However, by performing catalytic tests in a continuous reaction system, it was possible to observe the instability of the catalyst and to correlate it with Mg leaching from the support in aqueous medium. Based on ICP analysis and pH measurements, it was evidenced that an in situ homogeneous base formation was taking place because of support dissolution under hydrothermal conditions. If, on the one hand, the basic environment would contribute to the catalytic activity in a batch reactor, on the other hand, the catalyst deactivates faster in a CSTR regime. Ultimately, this work provides evidences that the use of catalysts based on HT supports should not be considered as base-free catalysis promoters under the aforementioned hydrothermal conditions.

4. Materials and Methods

4.1. Hydrotalcite Supports Preparation

Hydrotalcite samples (HTs) were prepared by co-precipitating aqueous solutions of Mg and Al salts as precursors with a highly basic solution [18]. Different molar ratios Mg: Al (2:1, 3:1, 4:1 and 5:1) were used to prepare the supports noted HT 2:1, HT 3:1, HT 4:1 and HT 5:1, respectively. The precursors solution ($\text{Mg}(\text{NO}_3)_2 \cdot 6 \text{H}_2\text{O}$ and $\text{Al}(\text{NO}_3)_3 \cdot 9 \text{H}_2\text{O}$ dissolved in deionized H_2O) was added dropwise to 1 M NaOH and the pH was maintained in the range of 10.5 ± 0.1 . The temperature during the synthesis was $55^\circ\text{C} \pm 0.2$. The solution was stirred for one hour, keeping the temperature constant. Then, the suspension was filtered and the solid was washed with warm distilled water (50°C). The final solid was dried overnight at 100°C in an oven and then ground using a mortar. To transform HTs to mixed oxides, the samples were calcined at 500°C for 3 h under static air with a temperature ramp of 5°C min^{-1} . Finally, XRD analyses were carried out to verify the crystalline structure of the samples.

4.2. Gold NPs on Hydrotalcite Supports

The 2 wt.% Au/HTs catalysts were prepared by a sol immobilization method using NaBH_4 and polyvinyl alcohol (PVA) as reducing and dispersing agents, respectively. The gold nanoparticles were prepared following the method described by N. Dimitratos et al. [20,21]. First, a 2% wt.% solution of PVA in distilled water was prepared (PVA/Au (*w/w*) = 1.2). When PVA was completely dissolved, this solution was added to an aqueous solution of $\text{HAuCl}_4 \cdot 3\text{H}_2\text{O}$ ($5.08 \times 10^{-4} \text{ mol L}^{-1}$) under vigorous stirring. A fresh NaBH_4 solution (0.1 mol L^{-1}) was prepared to yield a molar NaBH_4 to Au ratio of 5 and then added to the previous solution in order to form the metallic sol. The color of the sol was deep purple. After 30 min of sol generation, the gold nanoparticles were immobilized by adding different supports under vigorous stirring. The amount of support was calculated to give a final theoretical gold loading of 2 wt.%. After 2 h the slurry was filtered, the solid washed 3 times with 50 mL of warm water (50°C) and 50 mL of ethanol and further dried in oven at 100°C for 1 h. The solids obtained were

finally grinded to get the catalysts noted Au/HT 2:1, Au/HT 3:1, Au/HT 4:1 and Au/HT 5:1. With this preparation method, it was expected to obtain very small gold nanoparticles, with a diameter around 2–4 nm.

4.3. Catalysts Characterization

The X-ray diffraction (XRD) measurements of the solids were performed using a Bruker D8-Advance Powder X-ray diffractometer (Billerica, MA, USA). The patterns were obtained using CuK α radiation with an accelerating voltage of 40 kV and an emission current of 40 mA. The samples were scanned over a 2θ range of 10° to 70° , with a step size of 0.014° and a time of 19.2 s per step. Gold amount on each catalyst was determined by ICP-OES from Agilent Technologies (Santa Clara, CA, USA). A Vulcan 42 S—Questron Technologies/Horiba automated digester was associated to ICP to digest the powder catalysts precisely. For digestion, 2 mL of aqua regia was added to 5 mg of solid and heated to 65°C for overnight. For Transmission Electron Microscopy (TEM) analysis, the catalysts were dispersed in ethanol and left for 10 min in the ultrasonic bath. The instrument used was a TEM/STEM FEI TECNAI F20 microscope combined with an Energy Dispersive X-ray Spectrometer (EDS) (Hillsboro, OR, USA) at 200 kV. To calculate the average gold nanoparticles size, the diameters of 100 particles were measured from TEM images and used for statistics. Nitrogen adsorption and desorption analysis on the different catalysts were performed using a TriStar II Plus analyzer (Norcross, GA, USA) (Micromeritics). The samples were subjected to a pretreatment before the analyses to eliminate impurities that were adsorbed on the surface. Namely, the samples were heated to 250°C with a temperature ramp of $10^\circ\text{C min}^{-1}$ and then maintained at this temperature for 60 min under vacuum. To determine the total surface area of the analyzed catalysts, the BET model was used. The pore volume was also calculated using the BJH method. The total acidity or basicity of the catalysts was determined using a TPD/TPR/TPO Micromeritics instrument equipped with an MKS MS Spectrometer (Norcross, GA, USA). Generally, 15–30 mg of catalyst were pretreated up to 500°C (calcination temperature of the samples) under helium flow. For the NH_3 -TPD and CO_2 -TPD experiments, the samples were cooled to 50°C and 40°C , respectively, and the adsorption of each considered probe molecule was performed for 1 h flowing a mixture of 10% NH_3 or 10% CO_2 in helium. Then, helium was flowed for 30 min at the adsorption temperature to remove the excess of physisorbed molecules. Finally, the temperature was increased to 500°C ($10^\circ\text{C min}^{-1}$) and maintained at this temperature for 1 h.

4.4. Catalytic Tests

The catalytic tests were performed in a Top Industry autoclave. The reactant solutions were prepared by diluting a certain amount of furfural in 21 mL of H_2O , giving the desired concentration, and stirring the solution to dissolve furfural before adding it into the vessel. Starting solution (1 mL) was taken off for HPLC analysis, and the amount of catalyst, or bare support, (around 100 mg) was added in the autoclave. The reactor was purged three times with pure oxygen before reaching the pressure. After reaching 6 bar, the heating system was turned on. The first 10 min, to reach the desired temperature, were not considered in the reaction time and the final solutions were discharged only at the end of the reactions. All tests were carried out under uncontrolled pH conditions. At the beginning and at the end of the catalytic tests, the pH was measured. At the end, the reactor was cooled by an external air cooler system. The reaction mixtures were filtered, and 1 mL of the final solutions were diluted for HPLC analysis in a Phenomenex column (ROA, organic acid H^+ ; 300×7.8 mm). Sulphuric acid (5 mmol L^{-1}) was used as a mobile phase with a flow rate of 0.60 mL min^{-1} , and the products were detected on a Shodex RI-101 and UV-Vis detectors at 253 nm.

For the stability test, a continuous reaction system composed of a Parr reactor coupled to an Eldex reciprocating piston pump was employed, composing a CSTR-like system. First, 20 mL of a 2.5 gL^{-1} of furfural solution (FF/Au = 50) was added to the vessel together with 100 mg of Au/HT 4:1. The reactor was pressurized with 5 bar of synthetic air before turning the heating on. Finally, when the desired temperature (110°C) was reached, the stirring was turned on and a freshly prepared 2.5 gL^{-1} furfural

solution started to be pumped into the vessel at a flow rate of 0.5 mL min^{-1} . A collector equipped with a filter was dipped into the reaction medium to draw the liquid inside the vessel avoiding any catalyst removal. The outflow is controlled by a valve at around 0.5 mL min^{-1} to keep a constant volume of liquid in the reactor (steady state). The final pressure in steady state was around 6 bar. Furfural and furoic acid were quantified by HPLC as described before.

Supplementary Materials: The following are available online at <http://www.mdpi.com/2073-4344/10/1/73/s1>, Figure S1: TPD-CO₂ of hydrotalcite samples.

Author Contributions: Conceptualization, F.C., S.P. and R.W.; methodology, F.D.; validation, F.D.; formal analysis, A.R. and Y.C.; investigation, A.R. and Y.C.; resources, R.W.; writing—original draft preparation, A.R.; writing—review and editing, Y.C., S.P. and R.W.; supervision, F.C., S.P. and R.W. All authors have read and agreed to the published version of the manuscript.

Funding: This research received no external funding.

Acknowledgments: The REALCAT platform is benefiting from a state subsidy administrated by the French National Research Agency (ANR) within the frame of the 'Future Investments' program (PIA), with the contractual reference 'ANR-11-EQPX-0037'. The European Union, through the ERDF funding administered by the Hauts-de-France Region, has co-financed the platform. Centrale Lille, the CNRS, and Lille University, as well as the Centrale Initiatives Foundation, are thanked for their financial contributions to the acquisition and implementation of the equipment of the REALCAT platform. Chevreul Institute (FR 2638), and Ministère de l'Enseignement Supérieur, de la Recherche et de l'Innovation are also acknowledged for supporting and funding partially this work.

Conflicts of Interest: The authors declare no conflict of interest.

References

1. Sousa-Aguiar, E.F.; Appel, L.G.; Zonetti, P.C.; do Couto Fraga, A.; Bicudo, A.A.; Fonseca, I. Some important catalytic challenges in the bioethanol integrated biorefinery. *Catal. Today* **2014**, *234*, 13–23. [CrossRef]
2. Dunlop, A.P. Furfural formation and behavior. *Ind. Eng. Chem.* **1948**, *40*, 204–209. [CrossRef]
3. Brownlee, H.J.; Miner, C.S. Industrial development of furfural. *Ind. Eng. Chem.* **1948**, *40*, 201–204. [CrossRef]
4. Mariscal, R.; Maireles-Torres, P.; Ojeda, M.; Sádaba, I.; Granados, M.L. Furfural: A renewable and versatile platform molecule for the synthesis of chemicals and fuels. *Energy Environ. Sci.* **2016**, *9*, 1144–1189. [CrossRef]
5. Asano, T.; Tamura, M.; Nakagawa, Y.; Tomishige, K. Selective Hydrodeoxygenation of 2-Furancarboxylic Acid to Valeric Acid over Molybdenum-Oxide-Modified Platinum Catalyst. *ACS Sustain. Chem. Eng.* **2016**, *4*, 6253–6257. [CrossRef]
6. Asano, T.; Takagi, H.; Nakagawa, Y.; Tamura, M.; Tomishige, K. Selective hydrogenolysis of 2-furancarboxylic acid to 5-hydroxyvaleric acid derivatives over supported platinum catalysts. *Green Chem.* **2019**, *21*, 6133–6145. [CrossRef]
7. Li, X.; Lan, X.; Wang, T. Selective oxidation of furfural in a bi-phasic system with homogeneous acid catalyst. *Catal. Today* **2016**, *276*, 97–104. [CrossRef]
8. Dunlop, A.P. Process for Manufacturing Furoic Acid and Furoic Acid Salts. U.S. Patent No. 2/407/066, 3 September 1946.
9. Tian, Q.; Shi, D.; Sha, Y. CuO and Ag₂O/CuO catalyzed oxidation of aldehydes to the corresponding carboxylic acids by molecular oxygen. *Molecules* **2008**, *13*, 948–957. [CrossRef] [PubMed]
10. Verdeguer, P.; Merat, N.; Gaset, A. Lead/platinum on charcoal as catalyst for oxidation of furfural. Effect of main parameters. *Appl. Catal. A Gen.* **1994**, *112*, 1–11. [CrossRef]
11. Verdeguer, P.; Merat, N.; Rigal, L.; Gaset, A. Optimization of experimental conditions for the catalytic oxidation of furfural to furoic acid. *J. Chem. Technol. Biotechnol. Int. Res. Process Environ. Clean Technol.* **1994**, *61*, 97–102. [CrossRef]
12. Douthwaite, M.; Huang, X.; Iqbal, S.; Miedziak, P.J.; Brett, G.L.; Kondrat, S.A.; Edwards, J.K.; Sankar, M.; Knight, D.W.; Bethell, D.; et al. The controlled catalytic oxidation of furfural to furoic acid using AuPd/Mg(OH) 2. *Catal. Sci. Technol.* **2017**, *7*, 5284–5293. [CrossRef]
13. Yuan, Z.; Wu, P.; Gao, J.; Lu, X.; Hou, Z.; Zheng, X. Pt/solid-base: A predominant catalyst for glycerol hydrogenolysis in a base-free aqueous solution. *Catal. Lett.* **2009**, *130*, 261–265. [CrossRef]

14. Gupta, N.K.; Nishimura, S.; Takagaki, A.; Ebitani, K. Hydrotalcite-supported gold-nanoparticle-catalyzed highly efficient base-free aqueous oxidation of 5-hydroxymethylfurfural into 2, 5-furandicarboxylic acid under atmospheric oxygen pressure. *Green Chem.* **2011**, *13*, 824–827. [[CrossRef](#)]
15. Tongsakul, D.; Nishimura, S.; Ebitani, K. Platinum/gold alloy nanoparticles-supported hydrotalcite catalyst for selective aerobic oxidation of polyols in base-free aqueous solution at room temperature. *ACS Catal.* **2013**, *3*, 2199–2207. [[CrossRef](#)]
16. Ferraz, C.P.; Zieliński, M.; Pietrowski, M.; Heyte, S.; Dumeignil, F.; Rossi, L.M.; Wojcieszak, R. Influence of Support Basic Sites in Green Oxidation of Biobased Substrates Using Au-Promoted Catalysts. *ACS Sustain. Chem. Eng.* **2018**, *6*, 16332–16340. [[CrossRef](#)]
17. Ferraz, C.P.; Da Silva, A.G.M.; Rodrigues, T.S.; Camargo, P.H.C.; Paul, S.; Wojcieszak, R. Furfural Oxidation on Gold Supported on MnO₂: Influence of the Support Structure on the Catalytic Performances. *Appl. Sci.* **2018**, *8*, 1246. [[CrossRef](#)]
18. Zhao, R.; Yin, C.; Zhao, H.; Liu, C. Synthesis, characterization, and application of hydrotalcites in hydrodesulfurization of FCC gasoline. *Fuel Process. Technol.* **2003**, *81*, 201–209. [[CrossRef](#)]
19. Wojcieszak, R.; Ferraz, C.P.; Sha, J.; Houda, S.; Rossi, L.M.; Paul, S. Advances in base-free oxidation of bio-based compounds on supported gold catalysts. *Catalysts* **2017**, *7*, 352. [[CrossRef](#)]
20. Dimitratos, N.; Lopez-Sanchez, J.A.; Morgan, D.; Carley, A.; Prati, L.; Hutchings, G.J. Solvent free liquid phase oxidation of benzyl alcohol using Au supported catalysts prepared using a sol immobilization technique. *Catal. Today* **2007**, *122*, 317–324. [[CrossRef](#)]
21. Ferraz, C.P.; Garcia, M.A.S.; Teixeira-Neto, É.; Rossi, L.M. Oxidation of benzyl alcohol catalyzed by gold nanoparticles under alkaline conditions: Weak vs. strong bases. *RSC Adv.* **2016**, *6*, 25279–25285. [[CrossRef](#)]



© 2020 by the authors. Licensee MDPI, Basel, Switzerland. This article is an open access article distributed under the terms and conditions of the Creative Commons Attribution (CC BY) license (<http://creativecommons.org/licenses/by/4.0/>).